Astron. Astrophys. 283, 1037–1045 (1994)

ASTRONOMY AND ASTROPHYSICS

Procedures for the interactive analysis of point sources from the ROSAT XRT/PSPC All-Sky Survey

T. Belloni, G. Hasinger, and C. Izzo

Max-Planck-Institut für extraterrestrische Physik D-85748 Garching bei München, Germany

Received 22 April 1993 / Accepted 25 September 1993

Abstract. The *ROSAT* mission performed the first imaging all-sky survey in soft X–rays (0.1 – 2.4 keV) in 1990–1991. During the survey, roughly 50000 sources were detected, most of them on a basis of only a few photons. The analysis of *ROSAT* all-sky survey point-source data involves additional complications when compared to the normal techniques used for pointed-observation data. The determination of the correct exposure time and the selection of the background region are examples of critical problems. A set of interactive techniques for the extraction of source and background photons is described. Preliminary results from the survey observation of the black-hole candidate LMC X–3 are presented.

Key words: methods: data analysis – surveys – space vehicles – X-rays: general

1. Introduction

The X–ray observatory *ROSAT* was launched on 1990 June 1. It consists of a large X–ray telescope (XRT) with two mutually exclusive imaging instruments in the focal plane, and an external smaller EUV telescope coaligned with the XRT (for a description of the mission, see Trümper 1983). During the period 1990 August–1991 January, with additional observation intervals in 1990 July, 1991 February and 1991 August, *ROSAT* performed a scanning survey with nearly complete sky coverage. The Position Sensitive Proportional Counter (PSPC) was used exclusively with the XRT for the survey providing the first imaging survey of the sky at 0.1 – 2.4 keV. Simultaneously, the WFC provided the first imaging survey of the sky at slightly lower energies. The main features of the PSPC are high sensitivity, low instrumental background, accurate spatial resolution and moderate spectral resolution (see Pfeffermann et al. 1986 for a more detailed description of the instrument, Snowden & Freyberg 1993, Plucinsky et al. 1993 and Snowden et al. 1994 for discussion of the non-cosmic background).

Send offprint requests to: T. Belloni

During the all-sky survey *ROSAT*, detected roughly 50000 soft X–ray sources (Voges 1992), with an average exposure time of ∼500 s. Because of the low background and relatively sharp point-response function of the *ROSAT* PSPC, most of the sources were detected with only a very small number ($\gtrsim 6$) photons, which rules out detailed timing and spectral analysis. Nevertheless, for a substantial number of sources, the production of spectra and light curves in addition to a standard detection procedure (which gives basic parameters such as position, count rate, and hardness ratios) is possible. The analysis, however, is complicated by the very nature of the all-sky survey, which introduces a number of difficulties not present in the case of a simple pointed observation, where a source is continuously in the field of view and nearly at the same place in the detector. Moreover, many problems which may have occurred during the observation period (such as attitude errors) must be determined directly from the data.

In this paper, we will concentrate on the problems arising from the structure of the survey data, presenting a series of interactive techniques and strategies which can fruitfully be applied for extracting spectra and light curves for point sources. To a certain extent, the same line of discussion can be followed for moderately extended sources. For a discussion of the analysis of highly extended sources and the diffuse X–ray background see Snowden et al. (1994). We will not consider the corrections for effects like telescope vignetting or shadowing from the PSPC window-support structures: for a discussion of these effects see Zimmermann et al. (1993), Schaeidt (1993), and Molendi et al. (1993).

Section 2 of this paper describes the geometrical structure of the all-sky survey. Section 3 presents the basic structure of the data available to the user. In section 4, the possible cases of time windowing of the observation are examined. Section 5 discusses attitude-solution errors during an observation and what is probably the main difficulty in survey point-source analysis: the calculation of the effective exposure times. In Sect. 6, the problems associated with proper background extraction are presented, and a suitable technique is described. In Sect. 7, the procedures are applied to the all-sky survey data of the black

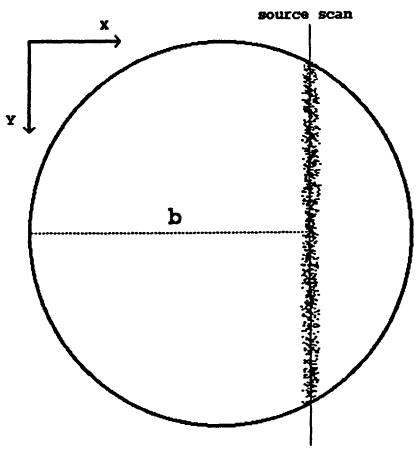

Fig. 1. A scan through the PSPC: the corresponding impact parameter b is marked

hole candidate LMC X–3. Finally, in section 8, we present a critical comparison between this method and others.

2. The All-Sky Survey

During the *ROSAT* all-sky survey, the satellite scanned the sky along great circles roughly perpendicular to the Sun position and which contained the ecliptic poles. Since, in the Earth reference system, the apparent motion of the Sun circles the Earth (and the satellite) with a period of 365 days, the entire sky can be covered after half a year. The scan period was synchronized with the orbital period of $\sim$ 96 minutes. The *ROSAT* PSPC has a circular field of view of 57′ radius. The time span over which a source was observed depended on the ecliptic latitude, β, of the source: a source on the ecliptic plane ($\beta = 0°$) was observed over $\sim$2 days, while a source located at one of the ecliptic poles ($\beta = \pm 90°$) was observed over the entire period of the survey. In the reference frame of the telescope during an orbit, a source scans along the Y-axis of the instrument for up to $\sim$30 s (see Fig. 1). The exact length of a scan depends on the "impact parameter," b, of the scan (for technical reasons, the impact parameter is measured as the perpendicular distance from the Y-axis in detector coordinates, which lies at one side of the detector, rather than from the center: see Fig. 1). Since the projected radius of the detector is 57′, and the scan speed is 3.75 arcmin s^{-1}, the duration of the longest scan is $\sim$ 30 s. The maximum exposure time for a source depends on the number of scans, determined by the ecliptic latitude of the source.

In reality, however, the instrument is switched off while the satellite enters the radiation belts or the South Atlantic Anomaly (see Snowden et al. 1992) and generally when there are satellite or detector failures. This means that sources can have missing or incomplete scans, or scans at widely varying times due to subsequent additional coverage at later times required to "fill in" major survey gaps. Another possible complication is introduced by scan reversals: every $\sim$30 days the direction of the scan rotation is reversed in order to avoid earth occultations. Depending on the source position, this might result in two consecutive scans over the source separated by a time larger or smaller than the 96-minute orbital/scan period. Finally, a key problem is the presence of attitude errors: the actual pointing direction of the satellite might not be the reported one in the aspect solution, and this might (or might not) be recorded in the attitude information provided with the data.

An important point to consider is that for survey data, the spatial and timing information are closely related: any time selection of photons is also a spatial selection (both on the sky and on the detector) and vice versa. As it will be discussed in section 6, correct techniques for the background subtraction are strongly dependent on this fact.

3. The structure of survey data

The all-sky survey data contain information about single detected photons, such as arrival time, pulse height amplitude, position in the detector and position in the sky, as reconstructed with the attitude solution. A list of "active times" is available, describing the time intervals when the detector was switched on and met operational criteria for acceptable data. These times are related only to the operations history, and give no information about whether a specific source was in the field of view.

An auxiliary file containing the attitude solution for the active time periods is also available. This file contains the position and orientation on the sky of the telescope field of view, with a time resolution of one second

As previously mentioned, the first and most crucial problem is to determine the correct accepted times for a given source, which is the intersection between the already available active times and the time intervals when the source was inside the field of view. Moreover, since the attitude solution might be incorrect during some intervals of time when the source was being observed, bad time intervals must be recognized and removed.

4. The impact parameter evolution

During each orbit, the instrument scans a region of the sky $\sim$ 2° wide and 360° long. Since all scans intersect each other at the ecliptic poles, the closer a source is to an ecliptic pole, the more scans will include it in the field of view: closer to the pole, the scans will be overlap to a greater degree, *i.e.*, the difference in impact parameter between consecutive scans will be smaller.

It is interesting to follow the nominal evolution of the impact parameter as a function of time for sources at different ecliptic latitudes. Let us examine several different cases:

- Source *at* the ecliptic pole: all the scans will be maximum scans, *i.e.*, the source always repeats the same scan passing through the center of the detector. The b *vs.* $< t >$ relation is always the same horizontal straight line.
- Source at low ecliptic latitude: the scans will be equally spaced with the distance between consecutive scans depending on the value of β. The scans will enter the detector from one side and leave it on the other. The b *vs.* $< t >$ relation is therefore a straight line with a slope depending on β. There is one exception: if the source happens to be in the field of view

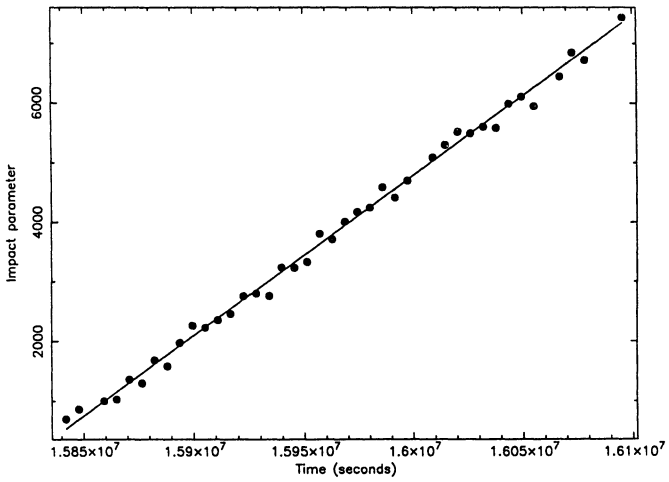

Fig. 2. Impact parameter evolution as a function of time for a low ecliptic latitude source. The continuous curve is a straight line fit to the data

at the beginning of the survey (with impact parameter b_0), it will leave the instrument in the way described above, but at the end of the survey it will re-enter the instrument from the same side, until the impact parameter reaches $b_{\max} - b_0$. The b *vs.* $< t >$ relation then consists of two separate straight segments with different slopes, separated by a long interval of time.

- Source within $\sim 2°$ from an ecliptic pole: this is the most complicated case. The relative number of sources fulfilling this criterion is low, but due to their long exposure, it will probably be worth analyzing all of them with this technique. As a good approximation (*i.e.*, neglecting curvature effects due to the projection of the celestial sphere on to the detector), the b *vs.* $< t >$ function will be an arc of a sinusoid, since it represents the linear projection of a point in circular motion. The period of the sinusoid is always 365 days (the time it takes for one complete circle), but the amplitude decreases for sources closer to the pole, and becomes 0 at the pole (see first case).
- It follows from the previous cases that for a "normal" source, that is a source away from the poles and the ecliptic, the impact parameter evolution will be an intermediate case. Since the curvature effects are proportional to $\frac{1}{\cos\beta}$, most of the cases will be similar to the one for low ecliptic latitude; only in a few cases will there be a significant deviation from a straight line. The user should note, however, that because of the multiple periods of survey operation (survey verification, main survey, and two periods of survey completion) and repeated coverage of certain regions during the main survey to fill in gaps, the observation intervals for some sources will be fragmented.

5. Determination of the exposure times

The source photons must be extracted by means of a spatial selection in sky coordinates. Given the properties of the PSPC point spread function and the techniques described below, a circular selection is most appropriate. The center and radius ξ of the circle can be estimated by looking at the photon radial distribution. A radius of $\xi = 400''$ has been found to be appropriate for sources with count rates smaller than $\sim$20 counts s^{-1} (Molendi et al. 1993). Of course, the extracted region will contain background photons as well, which have to be subtracted.

We have defined two basic approaches to the problem of the accepted times: they can be determined either from the photons or from the attitude solution. The first solution is less viable for weak sources, but if possible it is advisable to apply both: the comparison of the results can help in identifying attitude errors. The presence of background counts does not affect the present analysis, and in some cases it might turn out to be useful (see section 4.1). For reasons of simplicity, the photon approach is presented first.

5.1. Photon approach

Since the attitude information has already been used to reconstruct the position of the single photons in the sky, it is possible to use the photon data to estimate the accepted times. The main line of reasoning is straightforward: if a photon coming from the source position on the sky is detected (independent of whether it is actually from the source or from the background), the source position must be inside the detector field of view. The following is a step-by-step description of the algorithm:

- The first and last photons within a certain region of the sky from each scan are identified (this is trivial since events come in $\lesssim$ 30 s intervals separated by $\sim$ 96 minutes). The average between their arrival times, $< T >$, is taken as the central value for the scan interval (*i.e.*, the time when the source crosses the perpendicular to the Y–axis which runs through the center of the detector). If only one photon is found, its arrival time will be used as $< T >$. Scans with no photons will not be recognized at this stage.
- For each scan, the impact parameter, b, is determined by averaging the detector X coordinates of the single photons.
- At this stage, we should have a linearly decreasing/increasing function of b *vs.* $< T >$ (see Fig. 2). As we have seen in the previous section, however, this is not always the case. In the case where there are two or more separate intervals, the following procedures outlined here must be applied separately to each of the subsets. In the case of ecliptic polar sources, this method is *not* applicable and the attitude information has to be accessed directly (see following section).
- Because of photon statistics, there will be deviations from a straight line, particularly in the external scans where the vignetting function decreases and the scans become shorter. To correct for this effect, a linear least squares fit to the b *vs.* $< T >$ data should be performed, yielding a new set of "modified" $\tilde{b}$ values (see Fig. 2).
- It is now possible to recover scan intervals with no photons, providing they are not located at the beginning or at the end of the observation. If the time separation between

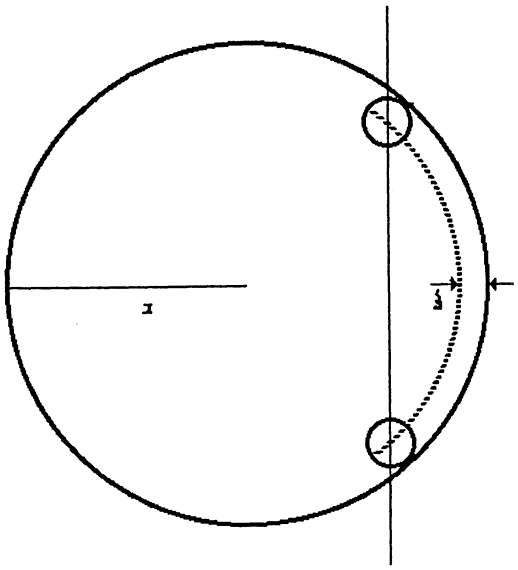

Fig. 3. Scan of a source extraction circle with radius ξ (see text)

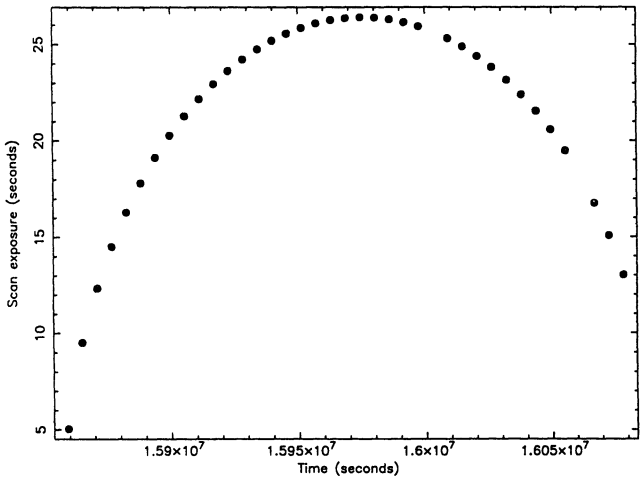

Fig. 4. Scan exposure time as a function of time corresponding to the impact parameters show in Fig. 2

two consecutive scans is significantly larger than 96 minutes (typically multiples of the orbital period), one or more empty scans are implied and can be tested for restoration. The original active-times information is checked to determine whether photons could have been detected. If this is the case (an exposed but empty interval), a new scan is added to the list. It will, of course, still contain no photons.

– Now that the central times of the scans are determined, as well as the impact parameter of the scan, the only missing information is the length (geometrical exposure) of each scan. In principle, the since the detector window is circular, the geometrical exposure corresponding to the sky position of the source (center of the extraction circle) can easily be determined. If b_c is the impact parameter corresponding to the central scan, we have:

$$\Delta t = \frac{2}{v} \times \sqrt{r^2 - (\tilde{b} - b_c)^2}$$

where $v = 3.75$ arcmin s^{-1} is the nominal scan speed and $r = 57'$ is the radius of the detector. However, it is necessary to include the non–zero extraction radius used. Without correcting for this effect, at the beginning and at the end of each scan there will be times when the source is inside the field of view, but only part of the extraction circle is exposed. The same applies to the most external scans, in which the extraction circle would never be completely in the field of view. To avoid these effects, only the times when the whole extraction circle is within the field of view should be used. To do this, an "effective" radius of the detector, $r_{eff} = 57' - \xi$, where ξ is the extraction radius, is defined (see Fig. 3). This procedure results in an exposure reduction at the extremes of each scan, and will occasionally eliminate a full scan at the beginning and/or end of the coverage of a source, but it ensures that only times with full exposure are used. The output of this procedure is the final list of time intervals contributing to the exposure (see Fig. 4). A time selection of the photons contained in these intervals will produce the appropriate photon list for subsequent analysis.

5.2. *Diagnostic of aspect–solution problems*

The photon approach has some disadvantages: it is in general advisable to check the results in order to identify (and correct) possible errors. These arise from the fact that the implied attitude information comes directly from the photons, whose distribution in time and space can introduce biases in the result. Obvious problems originate from the following:

– the fit to a straight line explicitly excludes regions of the sky where the deviations from a straight line are not negligible (see Sect. 4);
– the fit to a straight line also assumes that the scans are equally spaced in time. This is not always the case: not all the scans are exactly synchronized with the orbital period. In this case a time shift is introduced;
– another problem of the fit procedure arises when one or more scans are not located at the expected impact parameters, *i.e.*, one or more points significantly deviate from the expected curve. The fit procedure will incorrectly displace them;
– the start or the end of an active time period can happen while the source is in the field of view. In this case, the central time of the scan will not be calculated correctly, and therefore the exposure as well;
– because of the vignetting effects becoming larger at large off-axis angles, and because of the circular field of view, the external scans contain fewer photons than the central ones. The straight line fit is supposed to correct for this effect, but it is still advisable not to use the most external scans for the analysis.

The presence of these problems can be identified by looking at the b *vs.* $< T >$ and Δt *vs.* $< T >$ relations. Moreover, since

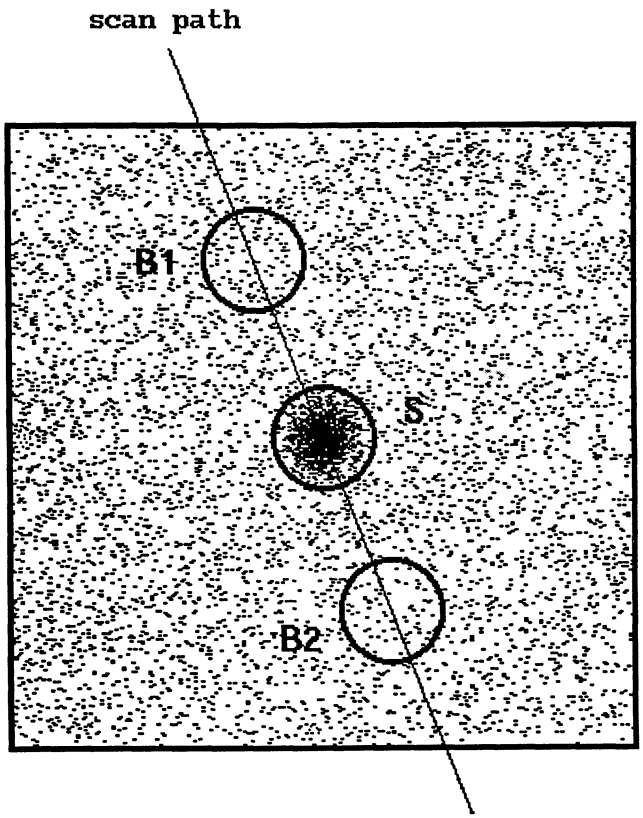

Fig. 5. Image in sky coordinates of the source extraction circle (S), and two background circles displaced along the scan direction (B1 and B2)

the attitude solution is available, it is possible to use it directly to derive the accepted times, and the results of the two methods should be compared

5.3. Attitude approach

The attitude solution gives the position in the sky of the optical axis of the instrument, sampled every second. It is possible from this to calculate the detector coordinates of the source position, independently of the presence of detected photons from that position. The idea is to read in the attitude information, compute the position of the source in the detector second by second, and use it as a "virtual photon". In this way, one has a constant 1 count s^{-1} source, unaffected by point spread function or vignetting effects. Then the algorithm described in the previous section can be applied. There are, however, two important differences:

1. Since the attitude solution is available for time intervals longer than the actual scan over the source, "photons" falling outside the 57′ field of view are also available. Therefore, it is possible to consider a square detector for the calculation of the impact time, avoiding sampling problems for the external scans.
2. No fit to the b *vs.* $< T >$ data is necessary.

The attitude approach is certainly safer than the photon one, but it might still be affected by errors caused by the inhomogeneity of the survey. Examining the b *vs.* $< T >$ and Δt *vs.* $< T >$ relations will help identify them. It is also advisable to apply the procedure described in the first half of this section and compare the results.

6. Extraction of background

The extraction of background photons for the production of net spectra and light curves is crucial for the proper analysis of point-source data. The usual approach of selecting background photons from an annulus around the source-extraction circle introduces unpredictable systematic errors in the determination of the background if the background is variable in time. In fact, even if the exposure time may be assumed with good approximation to be locally constant (*i.e.*, all the background area is exposed uniformly), it is also true that different points of the annulus are exposed at different moments in time. Points which are far from the source scan direction are exposed at much earlier or much later times, when the background level might have been different. In order to avoid this problem, the background area should be *always* defined along the source scan direction, and not too far from the source, in such a way that the background is always scanned just a few seconds before or after the source circle. The ideal choice would be a circle having the same radius as the source circle and whose center lies in the scan direction passing through the source position on the sky (see Fig. 5). The background exposure is naturally computed in the same way, i.e., independently from the exposure of the source (coverage from additional scans allowed for a background circle which lies closer to the nearest ecliptic pole than the source is excluded). This method holds even within the ecliptic pole regions. Also, since the scanning of the background region mimics the scanning of the source region, background subtraction becomes feasible also for the production of light curves. In order to avoid spurious effects due to the possible non-uniformity of the background, and to improve statistics, two (or more) such regions can be selected, half of them on one side (scanned before) and half on the other side (scanned after) of the source.

7. Observations

As an example of the application of exposure-time determination and background subtraction for the production of light curves and spectra, we present all-sky survey data from the black-hole candidate LMC X–3 (Cowley et al. 1983). The source is located in the Large Magellanic Cloud, and therefore lies close to the south ecliptic pole. This produced a considerably longer than average exposure. The source was in the field of view of the *ROSAT* PSPC both at the beginning and at the end of the survey: the observation window is thus split in two parts, roughly 6 months apart (see Sect. 4). For this reason, the attitude approach has been followed.

The source counts have been extracted from a circle of radius 500″, as determined by examining the radial profile of the detected counts. The source accepted times have been determined (see Sect. 5.3): the impact parameter evolution for the 70

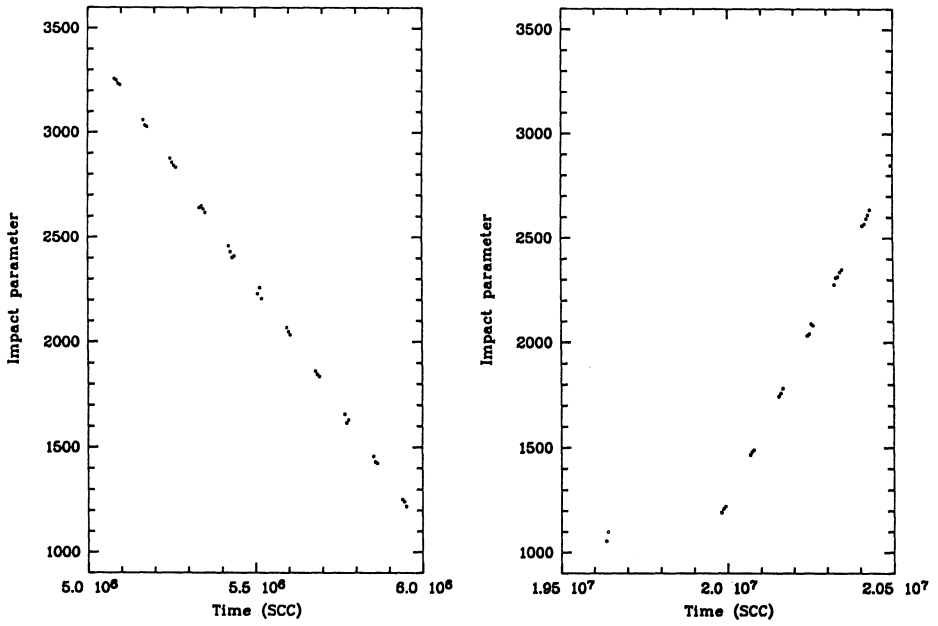

Fig. 6. Scan parameter evolution as a function of time for the source LMC X–3 (high ecliptic latitude)

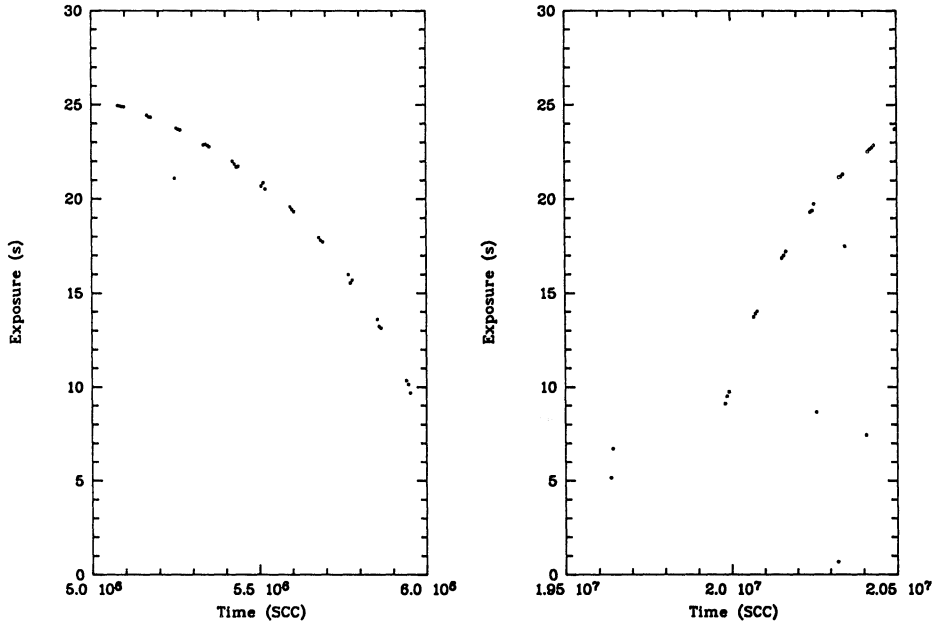

Fig. 7. Exposure times for LMC X–3 (see Fig. 6)

scans when the source circle was completely inside the detector is shown in Fig. 6. The two observation intervals have been separated for convenience of display. During the second interval, after the first two scans, the normal scan procedure was stopped to fill in some survey gaps caused by earlier operational failures; after that, the normal scan operation was restored. This effect shows up in Fig. 6 as a "break" in the second group of data. The periodic gaps every 24 hours are due to the switching off of the instrument because of the South Atlantic Anomaly and the southern particle belt. The corresponding exposure times are shown in Fig. 7. A few scans appear not completely exposed, and have been removed from the subsequent analysis. The first two isolated scans in the second window have also been removed. The remaining scans sum to a total exposure of 1180 seconds. The background photons have been extracted from two circular regions of radius 500″ displaced in the scan direction from the source position (see Sect. 6). Because of the high source count rate, however, the background subtraction is not critical.

Since the observation consists of separated groups of scans with a one-day period, a light curve has been produced by rebinning the data to have one point per day. The resulting net light curve, corrected for vignetting effects, is shown in the upper panel of Fig. 8. A monotonic increase in count rate by a factor of two is evident during the first observation interval, while six months later the count rate is substantially stable around 20 counts s^{-1}. The characteristics and the large amplitude of the variations exclude the possibility of spurious variability caused

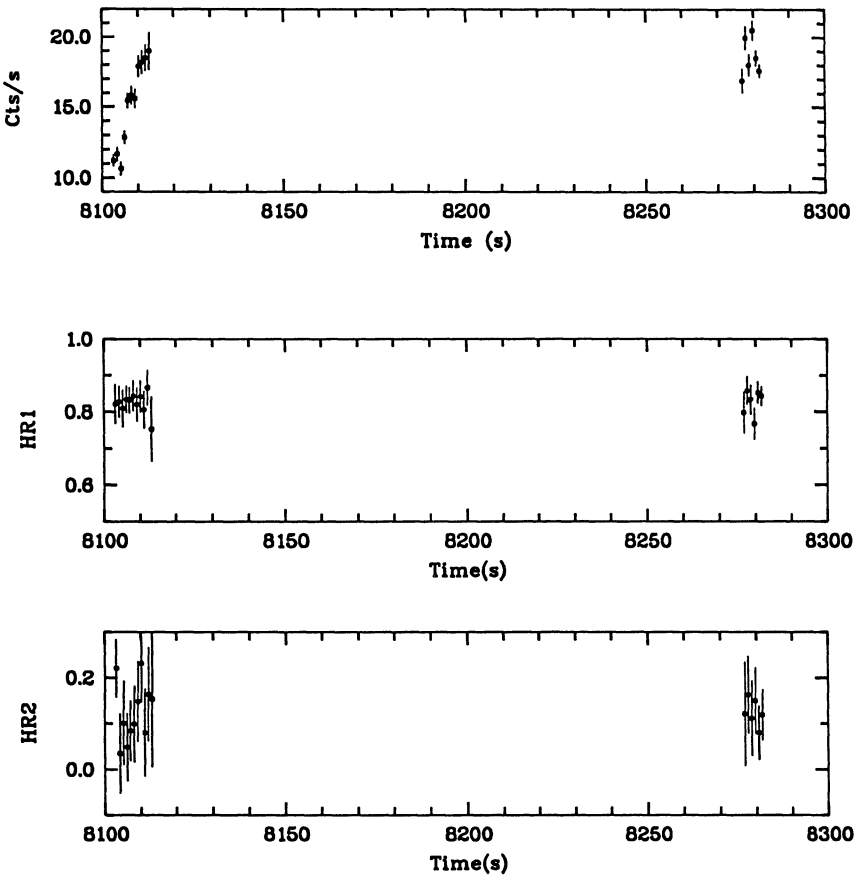

Fig. 8. Corrected count rate light curve of LMC X–3 (upper panel) and hardness ratio HR1 and HR2 light curves (lower panels). The hardness ratios are defined as: HR1=(D–C)/(D+C), HR2=(B–A)/(B+A), where the PHA channel intervals are A=8–40, B=41–240, C=41–100, D=101–240

by the shadowing of the PSPC support structures. The two standard PSPC hardness ratios (see caption of Fig. 8) show no variability within the errors, indicating the absence of significant spectral changes. The amplitude of the detected variability is common in the X–ray emission of LMC X–3 (Cowley et al. 1991): a change in spectral shape has been observed in the *Ginga* data, but given the much lower energy range of the PSPC, these changes are not expected to be visible in the *ROSAT* data.

The PSPC spectrum of LMC X–3, after subtraction of the background contribution, is shown in Fig. 9. Since no spectral variations were observed, all the data have been binned together. The data have been spectrally rebinned in order to locally oversample the energy resolution of the PSPC by a factor of three. A fit to a simple power law model (plus interstellar absorption) is acceptable, with reduced χ^2=1.3 for 16 d.o.f. (see Fig. 9). The value of the absorption, $N_H = (5.5 \pm 0.5) \times 10^{20}$ cm^{-2} (90% error), is lower than that estimated by EXOSAT (Treves et al. 1988a), but consistent with the reddening determined with IUE (Treves et al. 1988b). The photon index, $\Gamma = 1.43 \pm 0.09$ (90% error), is consistent with the value of 1.4 expected from the soft X–ray part of a Modified Disk Blackbody Spectrum with inner temperature kT$\sim$1 keV (Shakura & Sunyaev 1973). With the above spectral parameters, the 0.1–2.4 keV luminosity ranges from 0.7 to 1.5×10^{38} erg s^{-1} (assuming a distance of 55 kpc). A more complete analysis of the *ROSAT* data, including a series of pointed observations over a period of two years, will be presented elsewhere.

These results for LMC X-3 come from the application of the techniques described above to a bright X–ray source. An example of a weak source can be found in Finley et al. (1992). Other examples can be found in Molendi et al. (1993), Schaeidt et al. (1993) and Belloni et al. (1993).

8. Discussion

Any method applied to derive a background-subtracted spectrum from a source observed in the survey must solve three basic problems: the determination of the source exposure, the choice of the background area, and the determination of the background exposure. For deriving a background-subtracted light curve, the problem is essentially to choose the background area in such a way that the background light curve is taken almost simultaneously to the source light curve: we have seen that the only way to do so is to sample the background along the scan direction, as described in Fig. 5. The most crucial problem is therefore the determination of the source and the background exposure in the production of spectra.

The method presented in the previous sections is acceptable, both in the production of spectra and light curves, but only at the price of losing both exposure from each scan, and coverage (*i.e.*, scans at the beginning and at the end of the observation). In the example discussed in Sect. 7, there was a $\sim$ 37% loss from the available exposure time, and quite a few hours reduction in coverage. It is clear that in many cases, especially for weak

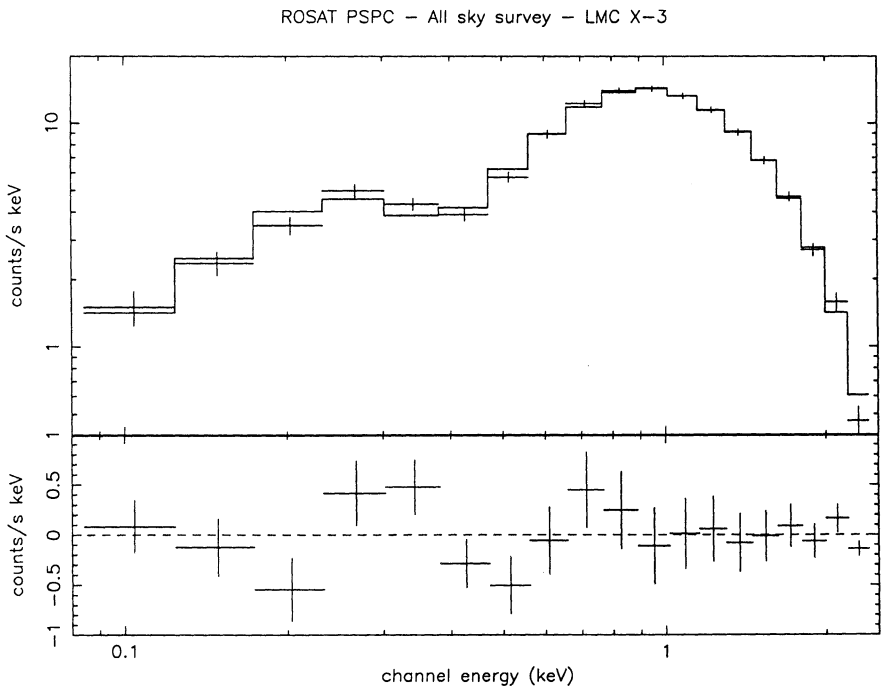

Fig. 9. Upper panel: PSPC count spectrum of LMC X–3, accumulated over the whole observation period. The line is the best fit to a power law model (see text). Lower panel: residuals after subtraction of the convolved model

sources, this method may not be acceptable (though there is really no other choice when extracting background subtracted light curves). However, we stress that only the lowest-quality data are lost, *i.e.*, those data at far off-axis angle which are strongly affected by vignetting, and perhaps more importantly, a significantly worse point response function.

In order to avoid photon loss in the production of spectra, some semi–automatic procedures, already available in some data analysis systems can be chosen.

In section 2 we have shown that, under the assumption of uniform survey (*i.e.*, no scans are missing), the exposure time for any point on the sky depends only on its ecliptic latitude. The uniform survey exposure time is proportional to $\frac{1}{\cos\beta}$ (up to $\sim 2°$ from the ecliptic poles), where the exposure becomes constant). It is easy to show that in selecting the source plus background photons from a $7'$ ring centered on the source, and the background photons within an annulus around the source with internal radius $7'$ and external radius $17'$, the error made by assigning to the background an exposure time equal to the central one is almost always negligible (under the assumption that the background is constant in time). In fact, even though there is always a gradient in the exposure within the background region because it covers points at different ecliptic latitudes, on average this effect is almost canceled by the linear symmetry of the problem. For a source located $\sim 3°$ from the ecliptic poles, where the exposure gradient is high, the error is about 0.2%. This is the method adopted for determining the exposure for the spectral extraction in the *ROSAT* PSPC Standard Analysis System (SASS, see Voges et al. 1992), where the source counts are extracted from a circle of radius $300''$ and the background from a ring with inner and outer radii $300''$ and $450''$ respectively (for the production of light curves, the background subtraction is not performed). But, as pointed out in Sect. 6, in case the assumption of background being constant in time is not correct, the determination of the background exposure is not sufficient. The choice of the background area should always be done as shown in Fig. 5, and not as an annulus, as it is necessary to avoid sampling for background subtraction regions of the sky which are far from the source scan direction and are therefore scanned at greatly different times.

Since the survey exposure is far from uniform, the analytical approach cannot be safely applied. Even neglecting its failure when working within ~ 3 degrees from the ecliptic poles, the required condition of (locally) uniform survey exposure fails (which is the most typical case) because of detector-off times due to passage of the satellite through Earth's particle belts and SAA. In the production of spectra, it is preferable to derive the exposure time from an *exposure map* (*i.e.*, a map containing the distribution of the geometrical exposures within the sky region under examination, see Snowden et al. 1994). The exposure at the source location and the *averaged* exposure over the area containing the background can then be computed, providing that the background is chosen along the scan direction in order to avoid problems from time variable background. This is probably the best available method. Of course, for each extraction of a spectrum from a specific time interval (within the observation time), a new exposure map must be created, a process which is generally quite time consuming. Moreover, if the exposure map is already corrected for the instrument response, as it normally is, it might be very difficult to derive the effective geometrical exposure of interest. It would be incorrect to avoid the problem by applying exposure and instrument correction together to both the source and the background spectra: since the instrument response is energy and position dependent, it cannot be assumed to be the same for the background and the source spectrum.

Within the X-ray data analysis package EXSAS (Zimmermann et al. 1993), the problem of the missing scans has been solved by accessing the attitude solution, and checking for the presence of the source within the detector frame during the observation time. Unfortunately this method is also not entirely satisfactory, since it is too sensitive to attitude errors and because the source stays within the detector for a short time, comparable with the sampling of the attitude solution. The uncertainties on the exposure times derived in this way can reach 5%. Moreover, in this case the computed (central) exposure must also be applied to the background counts, with all the limitations described above. Even if a complete set of basic tools for the production and the handling of survey light curves is available in EXSAS, no automatic data reduction procedure is yet supplied.

9. Conclusions

The analysis of point sources in the *ROSAT* XRT all-sky survey requires a number of special procedures for the determination of the exposure times and for the extraction of the source and background photons. Some specific interactive techniques have been presented. The preliminary results of the analysis of the all-sky survey data of the bright source LMC X–3 have been presented. The observed variability is consistent with previous X–ray observations of the source; the spectrum is consistent with a power law model, whose slope is in remarkably good agreement with the one expected from the soft X–ray part of a Modified Disk Blackbody spectrum with kT$\sim$1 keV.

Acknowledgements. We would like to thank all the ROSAT observers at MPE who have contributed to the testing of the analysis procedures. We thank S. Snowden for his critical reading of the manuscript.

References

Belloni, T., Hasinger, G., Pietsch, W. et al., 1993, A&A, 271, 487.
Cowley, A.P., Crampton, D., Hutchings, J.B. et al., 1983, Ap. J., 272, 118.
Cowley, A.P., Schmidtke, P.C., Ebisawa, K. et al., 1991, Ap. J., 381, 526.
Finley, J.P., Belloni, T., & Cassinelli, J.P., 1992, A&A, 262, L25.
Molendi, S., Maccacaro, T., & Schaeidt, S., 1993, A&A, 271, 18.
Pfeffermann, E., Briel, U.G., Hippmann, H. et al., 1986, SPIE, 733, 519.
Plucinsky, P.P., Snowden, S.L., Briel, U. et al., 1993, Ap. J., in press.
Shakura, N.I., & Sunyaev, R.A., 1973, A&A, 24, 337.
Schaeidt, S., 1993, PhD Thesis, Munich.
Schaeidt, S., Hasinger, G., & Trümper, J., 1993, A&A, 270, L9.
Snowden, S.L., & Freyberg, M.J., 1993, Ap. J., 404, 403.
Snowden, S.L., McCammon, D., Burrows, D.N., & Mendenhall, J.A., 1994, Ap. J., in press.
Snowden, S.L., Plucinsky, P.P., Briel, U., Hasinger, G. & Pfeffermann, E., 1992, Ap. J., 393, 819.
Treves, A., Belloni, T., Chiappetti L. et al., 1988a, Ap. J., 325, 119.
Treves, A., Belloni, T., Bouchet, P. et al., 1988b, Ap. J., 335, 142.
Trümper, J., 1983, Adv. Space Res., 2, no.4, 241.
Voges, W., 1992, ESA ISY–3, p.9.
Voges, W., Gruber, R., Paul, J. et al., 1992, ESA ISY–3, p.223.
Zimmermann, H.U, Belloni, T., Izzo, C. et al., 1993, "EXSAS User's guide", MPE Report 244.

This article was processed by the author using Springer-Verlag LaTeX A&A style file version 3.